Int. J. Heat Mass Transfer. Vol. 16, pp. 971–984 Pergamon Press 1973. Printed in Great Britain

# INCIPIENT-BOILING SUPERHEAT FOR SODIUM IN TURBULENT, CHANNEL FLOW: EFFECTS OF HEAT FLUX AND FLOW RATE*

**O. E. DWYER, G. STRICKLAND, S. KALISH, P. HLAVAC and G. A. SCHOENER**

Dept. of Applied Science, Bldg. 815, Brookhaven National Laboratory, Upton, N.Y. 11973, U.S.A.

(*Received* 18 *May* 1971 *and in revised form* 30 *August* 1972)

**Abstract**— An experimental study was carried out in which the effects of heat flux and velocity on the incipient-boiling superheat were determined for turbulent flow of sodium in an annular channel. The heating surface was polished type-316 stainless steel having a profilometer roughness of 14–18 μin. (rms). The rate of temperature rise of the heating surface was maintained constant in each incipient-boiling run, by gradually increasing the inlet sodium temperature to the test section, while the heat flux on the heater was held constant. In this way, the independent variables of heat flux and rate of temperature rise were separated.

For a finite rate of temperature rise, it was found that the greater the heat flux, the greater was the incipient-boiling superheat, other things being equal. It was also found that the greater the rate of temperature rise, the greater was the effect of heat flux. The flux was varied over the range 25 000–300 000 Btu/hft$^2$.

In general agreement with published results of previous investigators, the incipient-boiling superheat was found to have a strong dependence on the flow rate, falling off exponentially as the flow rate was increased.

The axial location of boiling inception was determined by means of a series of voltage taps spaced along the outer wall of the test section; and the results presented herein represent superheat values for, and nucleations at, the upper end of the heater, or at the highest heating-surface temperature in the test-section channel.

## NOMENCLATURE

$c_p$, specific heat [Btu/lb$_m$ °F];
$D_e$, $4m$;
$g_c$, conversion factor = 32·17 [lb$_m$ ft/lb$_f$ s$^2$];
$h$, heat transfer coefficient [Btu/h ft$^2$ °F];
IB, incipient boiling;
$k$, thermal conductivity of liquid [Btu/h ft °F];
$m$, (cross-sectional flow area)/(wetted perimeter) [ft];
$L$, heated length [ft];
$p$, vapor pressure of liquid [lb$_f$/in$^2$];
$p_L$, static pressure at nucleation site [lb$_f$/in$^2$];
$p_v$, vapor pressure of sodium (corresponding to $t_L$) at time of IB [lb$_f$/in$^2$];
$q$, heat flux at heating surface [Btu/hft$^2$];
$r$, bubble radius at boiling inception [in.];
$r_c$, radius of mouth of cavity [in.];
$r_1$, inner radius of annulus [in.];
$r_2$, outer radius of annulus [in.];
$R$, gas-constant = 1·987 Btu/lbmole°R];
$Re$, $D_e v\rho/\mu$ = Reynolds number [dimensionless];
$Re^*$, $Re$ corresponding to $y = y_{cr}$ [dimensionless];

* This work was performed under the auspices of the United States Atomic Energy Commission.

| | |
|---|---|
| $t$, | temperature [°F]; |
| $t_b$, | bulk temperature [°F]; |
| $T$, | temperature [°R]; |
| $t_{in}$, | temperature of inlet stream to test section [°F]; |
| $t_L$, | temperature of bubble at boiling inception [°F]; |
| $T_L$, | temperature of bubble at boiling inception [°R]; |
| $t_{sat}$, | saturation temperature [°F]; |
| $T_{sat}$, | saturation temperature [°R]; |
| $t_w$, | temperature of heating surface [°F]; |
| $T_w$, | temperature of heating surface [°R]; |
| $(t_w - t_{sat})^*$, | incipient boiling superheat corresponding to $r = r_c = y_{cr}$ [°F]; |
| $u^*$, | $\sqrt{(\tau_w g_c/\rho)}$ = friction velocity [ft/h]; |
| $v$, | average linear velocity [ft/h]; |
| $V_G$, | specific volume of vapor [$ft^3$/lbmole]; |
| $V_L$, | specific volume of liquid [$ft^3$/lbmole]; |
| $y$, | distance normal to heating surface [ft]; |
| $y^+$, | $yu^*/\nu$ = dimensionless distance normal to heating surface; |
| $y_{cr}$, | value of $y$ when $y^+ = 5$ [ft]; |
| $\theta$, | time [h]; |
| $\lambda$, | latent heat of vaporization [Btu/lbmole]; |
| $\mu$, | viscosity [$lb_m$/fth]; |
| $\nu$, | $\mu/\rho$ = kinematic viscosity [$ft^2$/h]; |
| $\rho$, | density [$lb_m/ft^3$]; |
| $\sigma$, | surface tension [$lb_f$/in.]; |
| $\tau_w$, | wall shear stress [$lb_f/ft^2$]. |

## INTRODUCTION

THIS paper presents results obtained in an experimental study of incipient-boiling (IB) superheats with sodium in turbulent flow. The effects of heat flux, linear velocity, and running time, on the magnitude of the superheat were determined, for flow in an annular channel with heat transfer from the inner wall only. This paper is a sequel to a previous one [1] in which the effect of rate of temperature rise (or temperature ramp) was covered. Each paper is based on a different portion of the same experimental study, where the equipment and general operating procedures were the same for both. Therefore, for detailed descriptions of these, the reader is referred to [1]. Briefly, the test section was about 3 ft long and consisted of a 0·52 in. dia. rod heater centered in a 0·93 in. i.d. tube. The heated length of the rod was 11·5 in.; the heating surface and remainder of the test section were made of type-316 stainless steel; the heating surface was polished to a toughness of 14–18 μin.; thermocouples were imbedded underneath the 0·013 in. thick cladding; and fully developed turbulent flow was obtained at the upstream end of the heated zone of the test heater.

All of the experimental results presented in this paper were obtained at a static pressure of 3·9 psia.

In forced-convection IB studies, it is possible to carry out the experiments in several different ways [1]. However, in most studies reported to date [2–4] with sodium, the inlet temperature to the test section and the flow rate are held constant, while the power to the test heater is applied in a single step. In this method, called method (c) in [1], the temperature of the heating surface goes through a transient. In their study with sodium, Logan *et al.* [5] fixed the inlet temperature and the flow rate, and then increased the power on the heater at a uniform rate over a very short period of time such that "the time period between the start of power increase and the onset of boiling was typically about 40 s." In that study, the temperature ramp was so high that it was of the same order as those in the experiments described in [2–4].

On the other hand, in the present study, the method of conducting an IB run was to maintain the heat flux and flow rate constant and increase the inlet temperature at a fixed rate.

This method, made possible by the use of a preheater, was called method (d) in [1].

In the experiments reported in [2–5], the temperature ramp, $\partial t_w/\partial \theta$, was coupled with the manner in, and the rate at, which the power on the test heater was increased. And Dwyer *et al.* [1] have shown experimentally that the temperature ramp during an IB experiment is a very important variable. Thus, in the abovementioned experiments, $q$ was not isolated and studied as an independent variable. In the present study, however, the independent variables of heat flux and temperature ramp were separated.

## TIME–TEMPERATURE TRACES

First of all, it is important to explain our definition of *boiling inception*, and what we looked for on the instrument recorders. In the first weeks of operation, we sometimes observed spikes on the temperature, pressure, and flowmeter charts, that lasted for a second or two. On the temperature ($t_w$) chart, there was an instantaneous and relatively large drop followed by a very quick recovery (Fig. 1). These so-called spikes rarely occurred more than two or three times during the heating-up period of a given run, and they showed no apparent tendency to come at either relatively low or high superheat levels. We discovered that these spikes could, for all practical purposes, be eliminated by subcooling the system after each run. For example, in the Series-6A runs*, this phenomenon was almost entirely eliminated. We suspect that it was caused by small uncondensed vapor pockets left behind after an IB event.

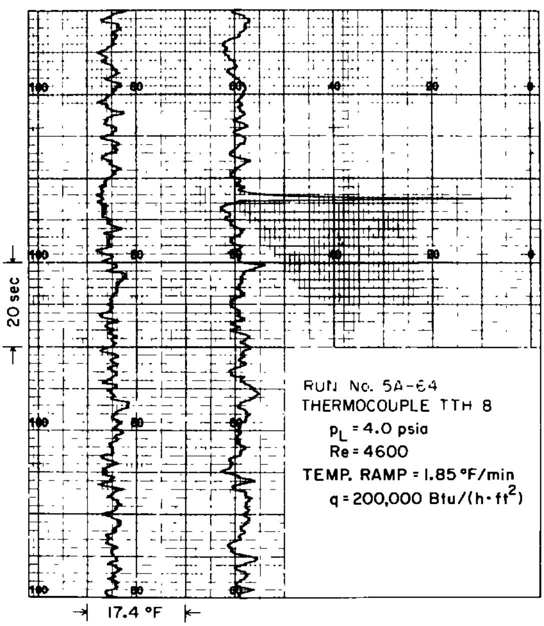


FIG. 1. Temperature trace (for a wall thermocouple near the axial location of boiling inception) that illustrates the occurrence of a low-temperature spike.

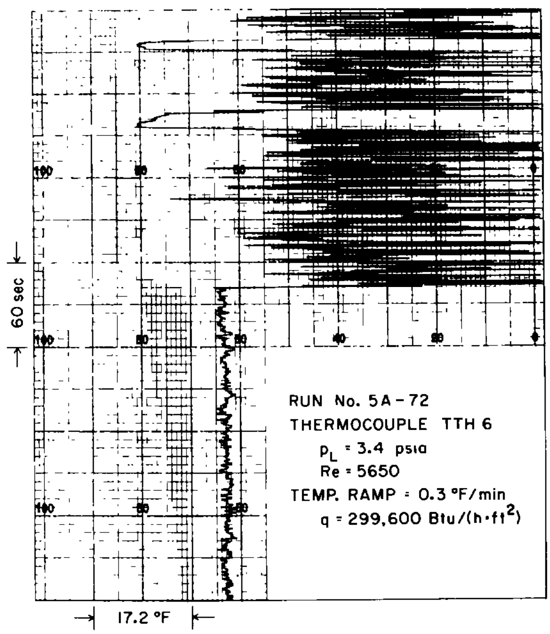


FIG. 2. Temperature trace (for a wall thermocouple near the axial location of boiling inception) that illustrates the onset and continuance of slugging, or unstable boiling.

Following nucleation, bubble growth was so rapid that the test section often became entirely filled with vapor, and the vapor pockets could have been formed on the test-section surfaces

* This paper is based on the results of two series, 5A and 6A.

during the subsequent, very rapid, re-entry of the liquid. These temperature spikes were, at no time during the study, taken to indicate the onset of boiling.

An IB event had to meet the following criteria in order to be counted: (1) there had to be at least 10 min of undisturbed temperature rise prior to the event, (2) there had to be at least one minute of continuous boiling after the event, and (3) in case boiling stopped, another boiling inception had to occur within 5 min. In some runs, the boiling (after IB) took the form of "slugging" (Fig. 2), when the pressure drop across the pump was not great enough. In at least 90 per cent of the runs, there was no temperature disturbance prior to inception, and

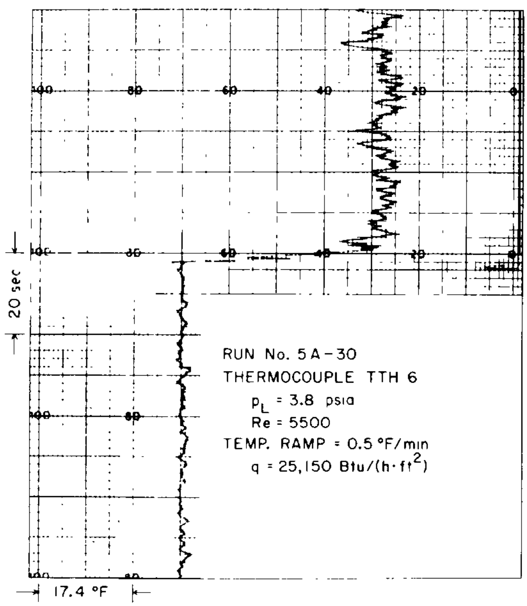


FIG. 3. Temperature trace (for a wall thermocouple near the axial location of boiling inception) that illustrates the onset and continuance of stable, forced-convection boiling.

the boiling that followed took the form of stable boiling (Fig. 3) and continued until the power on the test heater was shut off.

## EFFECT OF HEAT FLUX

*Review*

Hsu [6] was the first to produce a theoretical relation for predicting the effect of wall heat flux on IB superheat. Later, Bergles and Rohsenow [7] extended his concept and developed a relationship for forced-convection boiling of water that enabled one to predict the dependency of IB superheat on wall heat flux. We shall now examine the Hsu–Bergles–Rohsenow model and see why it is not applicable to liquid metals.

Nucleation occurs in small cavities in the heating surface, and the equivalent radii of such cavities for smooth surfaces generally lie in the range $10^{-6} \leqslant r_c \leqslant 10^{-3}$ in. This means that the hemispherical bubble shown in Fig. 4 lies well

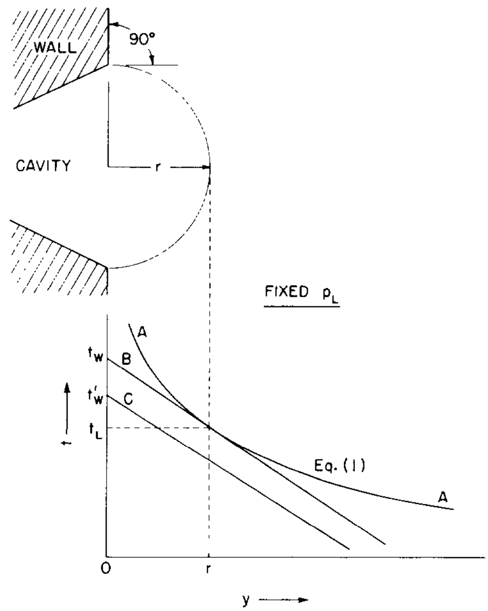


FIG. 4. Graphical illustration of the relationships between bubble radius, wall temperature, and heat flux at boiling inception, for an ordinary liquid.

within the so-called laminar boundary layer. Curve A represents the well known thermal-mechanical bubble equilibrium equation

$$p_v - p_L = \frac{2\sigma}{r} \tag{1}$$

for a spherically shaped interface, after $p_v$ is converted to $t$ by means of the vapor-pressure/temperature relationship for the liquid. Theoretically, an infinitesimal increase in $t$ would cause the bubble to grow and become unstable, thereby causing boiling inception. Line B in Fig. 4 represents the temperature gradient (in the liquid) normal to the wall and is given by the conduction equation

$$t = t_w - (q/k)\,y. \tag{2}$$

Line B is drawn tangent to curve A at $y = r$, which means that the temperature of the bubble decreases from $t_w$ at $y = 0$ to $t_L$ at $y = r$. This further means that the average temperature of the bubble is $>t_L$ and therefore more than adequate to produce bubble growth.

We have assumed that the presence of the bubble did not disturb the temperature pattern near the wall, which is probably not true; but the effect is a matter of considerable conjecture [8–10]. In view of this, Bergles and Rohsenow assumed that the temperature obtained from the point of tangency of curves A and B (in Fig. 4) closely approximated the minimum temperature required to produce bubble growth. A more realistic value of the wall temperature would probably be that indicated by $t'_w$ in Fig. 4 which would be obtained from a temperature line such as C, i.e. one having the same slope as that of B but giving an average, effective bubble temperature equal to $t_L$. But, the problem is that one does not know how to locate such a line.

We have also assumed that the heating surface contained an active cavity of radius $r$. If it did not, then IB would not occur at wall temperature $t_w$. Suppose the surface contained no potentially active cavities having effective bubble radii $\geqslant r$, then the next largest available cavity could be activated by raising the wall temperature by increasing $q$. This would call for the tangency of curves A and B occurring at some smaller value of $r$. Based upon this argument, Bergles and Rohsenow, and later, Sato and Matsumura [8], and Davis and Anderson [10] derived (by somewhat different assumptions and methods) analytical expressions for $(t_w - t_{sat}) = f(q)$ for water. These equations cannot be modified to work satisfactorily for liquid metals, as was first pointed out by Marto and Rohsenow [11]. This will now be discussed.

Let us look at Fig. 5, which is for a liquid metal. Curve A there represents a typical bubble-equilibrium curve, comparable to curve A in

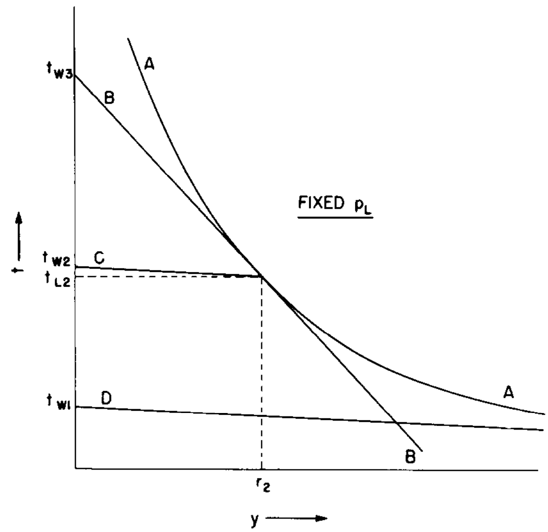


FIG. 5. Graphical illustration of the relationships between bubble radius, wall temperature, and heat flux at boiling inception, for a liquid metal.

Fig. 4. If we were to attempt to draw a conduction line tangent to curve A, we would find that the point of tangency would occur at a very large value of $y$ (or $r$). Curve D is such a line, and its point of tangency is beyond the scale of the figure. This happens because of the very high thermal conductivities of liquid metals, i.e. the conduction line is nearly horizontal.

It is obvious that if one were to apply the Hsu–Bergles–Rohsenow model to a liquid metal, it would yield an extremely large value of $r$ and a very low value of $(t_w - t_{sat})$, for boiling inception. Since liquid metals often wet solid metal surfaces extremely well, the larger cavities in a heat transfer surface are generally filled with liquid and are therefore inactive for nucleation purposes. Now, referring again to Fig. 5, suppose that $r_2$ is the radius of the largest available active cavity. Then, for the same heat flux, the surface temperature is now $t_{w2}$ at boiling inception. Also, because the conduction line is so flat, the wall temperature actually does not increase much for large increases in the wall flux; and therefore $(t_w - t_{sat})$ at IB does not change significantly for a considerable change in flux.

For the sake of illustration, heat-conduction curve B in Fig. 5 is drawn tangent to curve A at $y = r_2$ (as was done in Fig. 4), but in this case it represents an impossibly high heat flux.

It is thus apparent that the Hsu–Bergles–Rohsenow model, when adapted to liquid metals, would predict a negligible dependency of the IB superheat on wall heat flux. This can also be illustrated analytically, as follows.

The Clausius–Clapeyron equation can be written in the form

$$\frac{dp}{dT} = \frac{\lambda}{T(V_G - V_L)}. \tag{3}$$

Neglecting the specific volume of the liquid, and employing the perfect-gas law for the vapor, this equation becomes

$$\frac{dp}{p} = \frac{\lambda}{R}\frac{dT}{T^2}, \tag{4}$$

an approximate integration of which is

$$p_v - p_L = \frac{\lambda p}{RT^2}(T_L - T_{sat}), \tag{5}$$

where $\lambda p/RT^2$ is assumed constant over the temperature range $t_{sat}$ to $t_L$. Combining this with equation (1) gives

$$T_L - T_{sat} = \frac{2RT^2\sigma}{\lambda pr}. \tag{6}$$

If we now combine this equation with equation (2), replacing $T^2$ by $T_L T_{sat}$ and substituting $T_w$ for $T_L$, we end up with

$$t_w - t_{sat} = \frac{rq}{k} + \frac{2\sigma R T_w T_{sat}}{\lambda pr}, \tag{7}$$

where $\lambda$ may be evaluated at $(t_{sat} + t_w)/2$ and $p$ taken equal to $(p_v + p_L)/2$.

Equation (7) says that the wall superheat at boiling inception increases with an increase in $q$. But, $r/k$ is such a small number that the first term on the right-hand side of equation (7) is negligible compared to the second. This is the same as saying that, for liquid metals, line C in Fig. 5 is essentially horizontal, for any practical heat flux; and $(t_w - t_{sat})$ at boiling inception is, practically speaking, independent of heat flux. This, however, has not been borne out by the IB results reported for liquid metals (in channel flow) in the past, which have clearly shown that the IB superheat increases with increase in wall heat flux. For example, Peppler and Schultheiss [3] observed an average increase in $(t_w - t_{sat})$, at boiling inception, of $\approx 86$ °F ($\approx 65$ to $\approx 151$) for sodium, when the heat flux was increased from 203000 to 488000 Btu/hft$^2$. Also, Schleisiek [4] reported an average increase in $(t_w - t_{sat})$, at boiling inception, of $\approx 99$ °F ($\approx 113$ to $\approx 212$) for sodium, when the heat flux was increased from 600000 to 1190000 Btu/hft$^2$. And finally, Logan *et al.* [5] reported an average increase in $(t_b - t_{sat})$, at boiling inception, of $\approx 55$ °F ($\approx 40$ to $\approx 95$) for sodium, when the heat flux was increased from 300000 to 400000 Btu/hft$^2$, and for an inlet subcooling of 100 °F.

It has been suggested [12] that the observed heat-flux dependence of the IB superheat may be only apparent and most probably results from nucleation at rogue sites beyond the axial location of highest temperature in the test section. However, as will be shown later, the results of the present study do show that heat flux is an important independent variable, when inception occurs at the point of highest temperature in the test-section channel. An explanation of the discrepancy between experimental IB results and those predicted by the Hsu–Bergles–Rohsenow model will be offered later.

*Results*

Figure 6 presents some IB results for a temperature ramp of 0·7°F/min and for the other conditions listed on the figure. It is seen that the observed effect of heat flux is large. The figure shows all the data that were taken, i.e. no

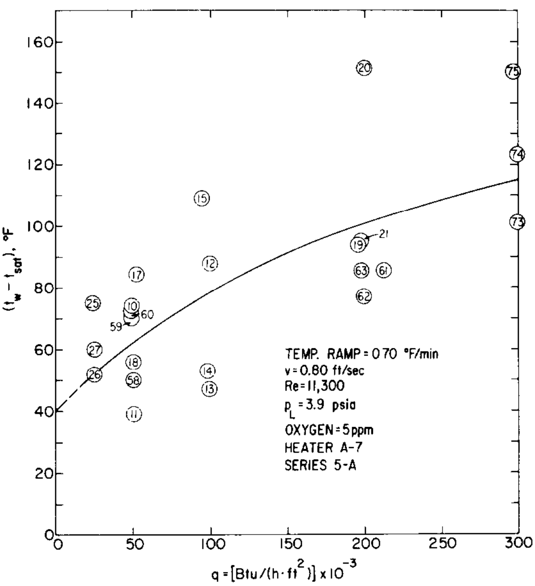


FIG. 6. Effect of wall heat flux on IB wall superheat for turbulent flow of sodium in an annular channel. Reynolds number equals 11 300.

points were discarded. As IB data for alkali metals generally run, those in Fig. 6 are fairly precise. When making the experimental runs, it was not always possible to hit the desired ramp just right. When that happened, the superheat was corrected to the reference ramp by means of the $(t_w - t_{sat})$ vs ramp curves shown in Figs. 3–5 in [1]. The curve in Fig. 6 was drawn "by eye" and, when extrapolated to zero heat flux, gave an IB superheat value of 40°F. For this limiting situation, the average deviation of the data is estimated to be $\pm 12°$.

Figures 3–5 in [1] show $(t_w - t_{sat})$ vs ramp curves for heat fluxes of 50000, 100000 and

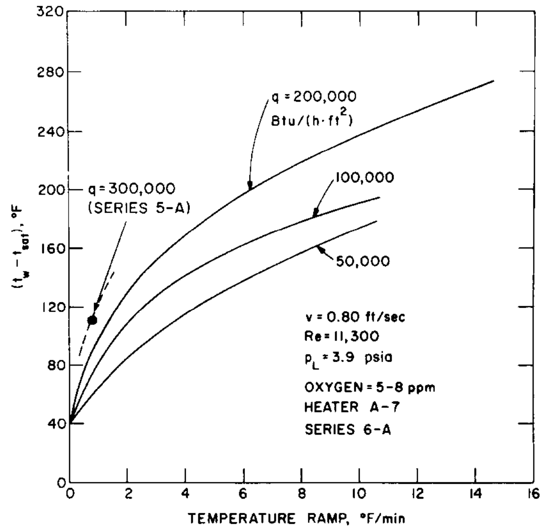


FIG. 7. Effect of rate of rise of wall temperature on IB wall superheat for turbulent flow of sodium in an annular channel, with wall heat flux as parameter. Reynolds number equals 11 300.

200000 Btu/hft$^2$, respectively. The precision of the data points in these figures is about the same as that in Fig. 6 herein. The curves in the three figures are reproduced in Fig. 7 in this paper, where it will be quickly noticed that as the temperature ramp approaches zero, the superheat, independent of heat flux, also approaches $\sim$40°F. By cross-plotting the curves in Fig. 7,

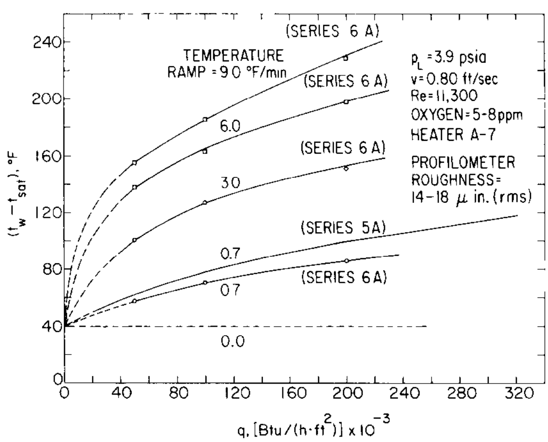


FIG. 8. Effect of wall heat flux on IB wall superheat for turbulent flow of sodium in an annular channel, with temperature ramp as parameter. Reynolds number equals 11 300.

and adding the curve in Fig. 6, we obtain the family of curves shown in Fig. 8. The symbols therein represent the values taken from the curves in Fig. 7. Even at finite temperature ramps, the results strongly suggest that, as the heat flux approached zero, the superheat approached a common value of $\sim 40°F$. In other words, as either the temperature ramp or the heat flux approached zero, the IB superheat approached $\sim 40°F$, for a flow rate of 0·80 ft/s, which is equivalent to a Reynolds number of 11 300.

The curves in Fig. 8 are, of course, uncertain at very low heat fluxes, particularly for the higher temperature ramps. That is why they are drawn dashed. It was not possible to obtain IB data at the very low heat fluxes due to the fact that rogue nucleation occurred either in the preheater or in the inlet region of the test section. It occurred in these places because of the relatively high temperature of the sodium leaving the preheater.

The main conclusion to be drawn from Fig. 8 is that the effect of heat flux on the IB superheat was found to vary with the temperature ramp—the smaller the ramp, the less the effect, until, as the ramp approached zero, the effect was negligible.

The two curves in Fig. 8 for a temperature ramp of 0·7 represent data taken at different times. The Series-5A data were taken during the period 11–17 December, while the Series-6A data were taken during the period 15–25 January. The total number of runs in each series was 66 and 84, respectively. There was no significant tendency for the superheats to change with passing of time in either series. A period of 28 days passed between the two series of runs, during which the loop was drained and maintained at room temperature, it was filled with argon under a pressure of 1·5 psig, and the sodium adhering to the test heater remained frozen. Thus, it is difficult to explain the difference between the two curves. Between the Series-5A and Series-6A runs, the oxygen content of the sodium increased from 5 to 8 ($\pm 1$) ppm. It is difficult to see how any of these changes could significantly affect the magnitude of the IB superheat. Increase in oxygen concentration has generally been found [5, 18] to decrease the superheat, but the difference between 5 and 8 ppm is not believed to be significant.

Inspection of the test heater, after completion of the experimental program, showed that the heating surface in the maximum-temperature zone had developed a crystalline appearance, although its profilometer roughness had remained unchanged. In the remainder of the heated zone, the original polished stainless-steel surface had developed a satin sheen.

Some investigators [3, 19] have found the IB superheat to increase with passing of time, for sodium in turbulent flow, while others [5] have found it to decrease. It can be postulated that in relatively short exposure times, depletion of gas from, and increased wetting of, heating-surface cavities could cause an increase in the IB superheat. On the other hand, in long-term exposures, pitting of stainless-steel surfaces with exposure of poorly-wetting nitrides and carbides at the grain boundaries could conceivably decrease IB superheats.

In the present study, over 100 IB runs had been made with the same heater prior to December 11, but the results were not worked up, for two reasons: (1) premature nucleation, apparently caused by the presence of gas, and (2) nucleation downstream from the end of the heated zone of the test heater. Extended operation took care of the first, and greater cooling beyond the heated zone of the test section took care of the second. During that break-in period, the short-term effects (mentioned above) had presumably disappeared.

*Discussion*

In the present study, temperature ramp and wall heat flux were, for the first time, separated as independent variables. This was done, in a given run, by fixing the flux and the flow rate, and then increasing $t_w$ (by increasing $t_{in}$) at a fixed rate, until IB occurred. This was referred to earlier as experimental method (d). This method contrasts with method (c), also described earlier, whereby the flow rate and inlet temperature are fixed and the power (corresponding to a given steady-state heat flux) is applied instantaneously to the heater. In this method—the one generally employed by investigators in the past—temperature ramp and heat flux are covariant.

a line does not give the effect of $q$ on $(t_w - t_{sat})$ at IB, when all other independent variables, including the temperature ramp, are held constant. According to the results of the present study, this would be given by an "incipient-boiling" curve, such as $\overline{fcg}$, where heat flux is the independent variable, and where pressure, velocity, and temperature ramp are held constant. By contrast, the heat-balance line $\overline{abcd}$, as

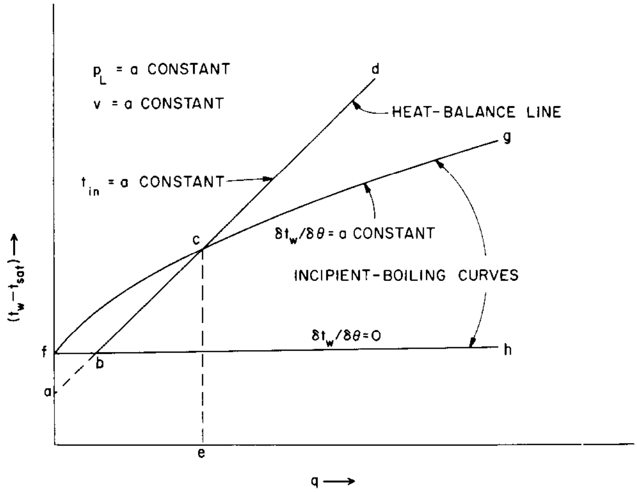


FIG. 9. Effect of wall heat flux on IB superheat, showing the relationship between a typical IB curve and a typical heat-balance line. The IB curve is a function of the rate of rise of the heating wall temperature; the heat-balance line is given by equation (8).

Let us now turn to Fig. 9. There, we see a heat-balance line, given by the equation

$$t_w - t_{sat} = q\left[\frac{1}{h} + \frac{2r_1L}{v\rho c_p(r_2^2 - r_1^2)}\right] + (t_{in} - t_{sat}), \qquad (8)$$

and two incipient-boiling curves—one for a finite temperature ramp, and the other for a ramp of zero. Equation (8) assumes negligible heat losses from the test section. Incipient-boiling measurements obtained by method (c) would fall along the portion $\overline{bcd}$ of the heat-balance line $\overline{abcd}$, if steady-state thermal conditions were approached by the time each IB event occurred, which is generally observed to be true, except at very high heat fluxes. But, such

equation (8) shows, represents fixed values of pressure, velocity, inlet temperature, and test-section geometry.

Still referring to Fig. 9, IB runs carried out by method (c) would give superheat values that would fall along the heat-balance line, if inception did not occur until steady-state conditions were approached. On the other hand, IB runs carried out by method (d) would give superheat values falling along the incipient-boiling curve, according to the results of the present study. For heat fluxes below that corresponding to point e, IB values by method (d) would be greater than those by method (c), and vice versa.

Referring back to Fig. 8, as either the heat flux or the temperature ramp approaches zero, the IB superheat approaches a lower limit of ~40°F; which indicates, that for very long waiting periods, the IB superheat is more equilibrium (than kinetics) controlled. However, there is still a velocity effect, as long as the flow is turbulent. Therefore, in order for equilibrium to be completely controlling, the flow should be laminar.

This all points to the conclusion that, if the flow is laminar, and if either the temperature ramp or the heat flux approaches zero, then the IB superheat should approach that given by equation (1), and the Hsu–Bergles–Rohsenow model would then be correct in predicting no significant effect of heat flux on IB superheats for liquid metals.

## EFFECT OF FLOW RATE

### *Review*

The general situation regarding the effect of flow rate on IB superheats for liquid metals is similar to that regarding the effect of heat flux. All of the experimental results that have been published to date [4, 5, 13, 14] show a strong effect of flow rate on the magnitude of the IB superheat, the superheat falling off exponentially with increase in flow rate. But, a generally acceptable explanation of the effect has not yet been found. Chen [15] suggested that the effect was probably due to pressure fluctuations at the heating surface caused by the stream turbulence; but Bankoff [16] showed by a random-walk theoretical analysis that, in order to explain the velocity effect in terms of local pressure fluctuations, the linear velocities would have to be at least an order of magnitude greater than those used in the experiments.

There is another phenomenon that could help to explain the velocity effect, and that is the existence of relatively large temperature fluctuations of the heating surface for heat transfer to liquid metals in turbulent, channel flow. Such fluctuations have been reported by Dwyer *et al.* [17] for mercury flowing inline through an unbaffled rod bundle. In the view of the present authors, it is possible that the combined effects of pressure fluctuations at the heated surface and temperature fluctuations of the heated surface could explain the often observed velocity effect. In other words, the coincidence of low-pressure and high-temperature "spikes" at a nucleation site could conceivably produce a rise in $p_v$ and a drop in $p_L$ (see equation (1)), such that the IB superheat is reduced appreciably below the laminar-flow value.

Pezzilli *et al.* [14] have proposed a mathematical model for predicting the effect of flow rate on IB superheat, that is based upon a number of assumptions. Among these, is the assumption that the heat of vaporization required for the explosive growth of the incipient bubble comes not only from the energy stored in the superheated liquid and the heating wall, but to a slight extent from the kinetic energy of the turbulent eddies as they slow up when they approach the outer bound of the laminar layer (i.e. at $y^+ = 5$). It is this energy that is claimed to trigger the inception. Another assumption is that the radius of the incipient vapor bubble decreases as it emerges (from the cavity) above the plane of the heating surface, reaching the radius of the cavity as the lower limit.

Pezzilli *et al.* assumed that the height, $y_{cr}$, of the (most stable) bubble sitting over an active cavity in the heating surface is equal to the classical laminar distance corresponding to $y^+ = 5$. When $y_{cr}$ equals the radius, $r_c$, of the mouth of the cavity, the IB superheat attains its maximum possible value. Thus, there is a critical Reynolds number, $Re^*$, that will give a $y$ $(=5\nu/u^*)$ value equal to $r_c$. At this Reynolds number and below, the IB superheat will be the same as that for pool or laminar flow boiling. In other words, $Re^*$ is the lowest Reynolds number for which there is a velocity effect on the IB superheat. As the Reynolds number increases above $Re^*$, $y$ will be less, $r$ will be greater, and the IB superheat will be lower, and therefore, the greater the Reynolds number the less will be the IB superheat. Through $y_{cr}$, Pezzilli *et al.* related $r$ (and therefore the IB superheat) to $Re$. It is not appropriate to take the necessary space here to give the derivation of their final correlating equation, which is

$$t_w - t_{sat} = \frac{2(t_w - t_{sat})^*}{\left(\frac{Re^*}{Re}\right)^{\frac{7}{8}} + \left(\frac{Re}{Re^*}\right)^{\frac{7}{8}}}, \qquad (9)$$

where $(t_w - t_{sat})^*$ corresponds to the maximum IB superheat, corresponding to $r = r_c = r_{cr}$.

*Results*

Unfortunately, the present study was ended before a good amount of data showing the effect of flow rate on IB superheat was obtained. However, they are worth showing, because they are the first such data that were obtained under conditions where the axial location of nucleation was rather carefully measured. The experimental results are shown in Figs. 10 and 11, for heat fluxes of 50000 and 200000 Btu/hft$^2$, respectively. Although the actual data points are few, the large effect of flow rate on the superheat is unmistakably evident.

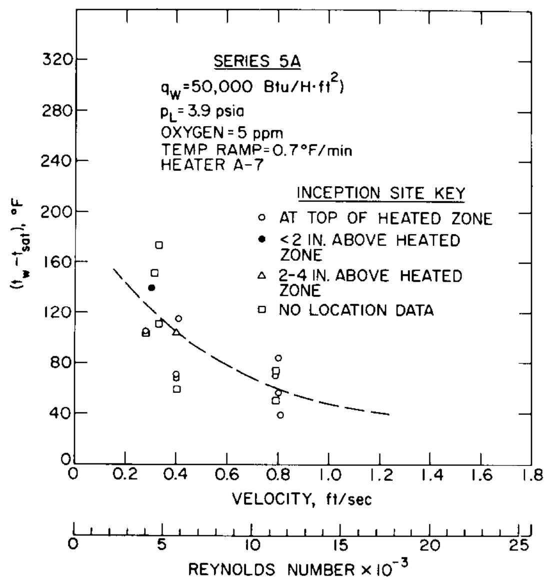


FIG. 10. Experimental results showing the effect of flow rate on incipient-boiling superheat, for sodium in turbulent, channel flow. Heat flux = 50000 Btu/hft$^2$.

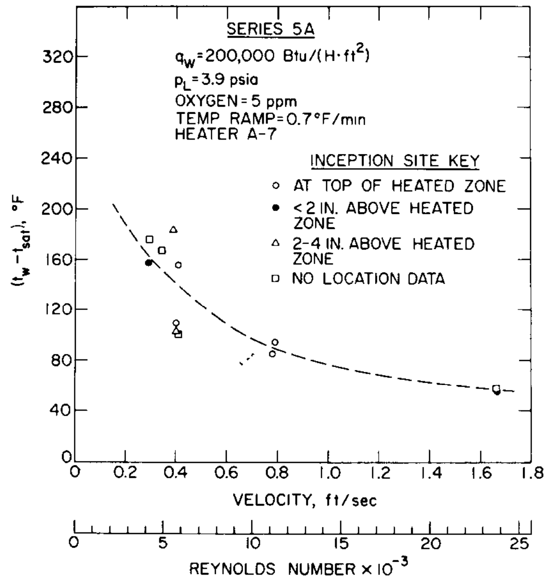


FIG. 11. Experimental results showing the effect of flow rate on incipient-boiling superheat, for sodium in turbulent, channel flow. Heat flux = 200000 Btu/hft$^2$.

In both figures, $(t_w - t_{sat})$ represents the superheat at the highest temperature of the heater, even though in some cases, nucleation was found to occur two or more inches downstream from that point. The curves shown on the figures were drawn simply by sight and are considered to be only approximate.

*Discussion*

In both Figs. 10 and 11, there are several data points for Reynolds numbers in the vicinity of 5000, for runs where IB occurred slightly downstream from the end of the heated zone, or where the axial location of inception was not measured. In those cases, we can say that the $(t_w - t_{sat})$ values shown are at least as great as, and probably somewhat less than, the $(t_w - t_{sat})$ values would have been, had IB occurred at the highest-temperature point. In other words, the true velocity effect was at least as great as that indicated on the plots.

Table 1 presents a comparison of the present IB superheat results on sodium with those published by Pezzilli *et al.* [14]. Those published by Schleisiek [4] and by Logan *et al.* [5], although clearly showing a strong dependence on flow rate, exhibited so much scatter of the data points that the present authors hesitated to draw curves through them. The observed superheats at four different Reynolds numbers are given in the table under item 6. A direct comparison between the Pezzilli results with those of the present study is not possible, because both the surface roughness and heat flux in the Pezzilli study are not known. Moreover, Pezzilli *et al.* made their IB runs by method (c), while the present authors made theirs by method (d). Also, owing to the scarcity of data points at the low Reynolds numbers, the values of $(t_w - t_{sat})^*$ and $Re^*$ for the present results must be considered approximate.

Whether or not the model of Pezzilli *et al.* is correct, equation (9) can be used to correlate IB superheat data. But, unfortunately, the quantity $(t_w - t_{sat})^*$ must be obtained from pool-boiling data on the same heating surface that was used to obtain the forced-convection data. A more practical approach is to evaluate $(t_w - t_{sat})^*$, $Re^*$, and the exponent directly from the forced-convection data to be correlated. When that was done for the Pezzilli results and those of the present study, the results shown under item 7 in Table 1 were obtained.

The quantity $(t_w - t_{sat})^*$ theoretically represents the value of the IB superheat at $0 \leqslant Re \leqslant Re^*$, and the values of $(t_w - t_{sat})^*$ in the table are consistent with the superheat values given under item 6. The $Re^*$ values also look quite reasonable. Moreover, the values of the exponent are not greatly different from each other or from the theoretical value of $\frac{7}{8}$ in equation (9), as originally proposed by Pezzilli *et al.* [14]. Since the value of the exponent indicates the IB dependency on the Reynolds number, we can conclude (allowing for the scatter of the data) that the effect of flow rate on the IB superheat observed in the present study was very similar to that found by Pezzilli *et al.*

## REFERENCES


1. O. E. DWYER *et al.*, Incipient-boiling superheats for sodium in turbulent, channel flow: effect of rate of temperature rise, *J. Heat Transfer* (accepted for publication).
2. L. FALZETTI *et al.*, Sodium boiling experiments: liquid superheat results under forced convection, CNEN Report RTI/TS(69)2 Centro Di Studi Nucleari, Della Casaccia, Italy (April 1969).
3. W. PEPPLER and G. F. SCHULTHEISS, Liquid-metal boiling research, Rept. Nos. KFK874 and EUR 4157e, Kernforschungszentrum, Karlsruhe (October 1968).
4. K. SCHLEISIEK, Heat transfer and boiling during forced convection of sodium in an induction-heated tube, *Nucl. Engng Design* **14**, 60–68 (1970).
5. A. D. LOGAN, C. J. BAROCZY, J. A. LANDONI and H. A. MOREWITZ, Effects of velocity, oxide level, and flow transients on boiling initiation in sodium, in *Liquid-Metal Heat Transfer and Fluid Dynamics*, pp. 116–28. ASME Symposium volume (30 Nov. 1970).


*Table 1. Comparison of experimental data on the effect of flow rate on the magnitude of the incipient-boiling superheat for sodium*

| | | | |
|---|---|---|---|
| 1. Investigators | Pezzilli *et al.* [14] | Present study | Present study |
| 2. Heating surface | stainless steel | 316 s.s. | 316 s.s. |
| 3. Surface finish | smooth, "as received" | polished, 14–18 μin. (rms) | polished 14–18 μin. (rms) |
| 4. $p_L$ (psia) | 6·5–9·0 | 3·9 | 3·9 |
| 5. $q$, (Btu/hft$^2$) | ? | 50000 | 200000 |
| 6. I.B. superheat (°F) | | | |
| a. at $Re = 5000$ | 106 | 113 | 151 |
| b. at $Re = 10000$ | 75 | 68 | 97 |
| c. at $Re = 20000$ | 40 | (38) | 63 |
| d. at $Re = 40000$ | 15 | — | — |
| 7. Constants in equation (9) | | | |
| a. $(t_w - t_{sat})^*$ (°F) | 121 | 140 | 180 |
| b. $Re^*$ | 3000 | 2500 | 2500 |
| c. Exponent | 1·07 | 0·99 | 0·89 |

6. Y. Y. HSU, On the size range of active nucleation cavities on a heating surface, *J. Heat Transfer* **84**, 207–16 (1962).
7. A. E. BERGLES and W. M. ROHSENOW, The determination of forced-convection surface-boiling heat transfer, *J. Heat Transfer* **86**, 365–72 (1964).
8. T. SATO and H. MATSUMURA, On the conditions of incipient subcooled boiling with forced convection, *Bull. JSME* (*Japan Soc. Mech. Engrs.*) **7**, 392 (1964).
9. D. B. R. KENNING and M. G. COOPER, Flow patterns near nuclei and the initiation of boiling during forced-convection heat transfer, in *Proc. Symp. Boiling Heat Transfer in Steam-Generating Units and Heat Exchangers*, Vol. 180, Pt. 3C, pp. 112–23 (1965–66).
10. E. J. DAVIS and G. H. ANDERSON, The incipience of nucleate boiling in forced-convection flow, *A.I.Ch.E. Jl* **12**, 774–80 (1966).
11. P. J. MARTO and W. M. ROHSENOW, Effect of surface conditions on nucleate pool boiling of sodium, *J. Heat Transfer* **88**, 196–204 (1966).
12. H. K. FAUSKE, R. E. HOLTZ and R. M. SINGER, The apparent effect of velocity upon liquid–metal boiling inception, *Trans. A.N.S.* **14**, 238–239 (1971).
13. J. C. CHEN, An experimental investigation of incipient vaporization of potassium in convective flow, in *Liquid–Metal Transfer and Fluid Dynamics*, Annual Meeting of ASME, New York. Symposium Volume, 129–34. (30 Nov. 1970).
14. M. PEZZILLI, A. SACCO *et al.*, The NEMI model for sodium boiling and its experimental basis, *ibid.*, pp. 153–61.
15. J. C. CHEN, Effect of turbulent flow on incipient-boiling superheat. Summaries of Presentations from First Meeting, Technical Working Group on Liquid–Metal Thermal Science, Brookhaven National Laboratory (May 1969).
16. S. G. BANKOFF, A random-walk theory for the inception of bubble growth in flowing liquid metals at a heated wall, Paper No. 28, presented at the 1971 International Heat Transfer Seminar (Heat Transfer in Liquid Metals), Trogir, Yugoslavia (6–11 September 1971).
17. O. E. DWYER, P. J. HLAVAC and M. A. HELFANT, Heat transfer to mercury flowing in-line through an unbaffled rod bundle: effect of rod displacement on local surface temperature and local heat flux, *Nucl. Sci. Engng* **41**, 321–35 (1970).
18. G. F. SCHULTHEISS, Experimental investigation of incipient-boiling superheat in wall cavities, *Liquid–Metal Heat Transfer and Fluid Dynamics*, ASME Symposium Volume, pp. 100–107 (30 Nov. 1970).
19. W. PEPPLER and E. G. SCHLECTENDAHL, Experimental and analytical investigations of sodium boiling events in narrow channels, *ibid.*, pp. 162–78.

## SURCHAUFFE EN DEBUT D'EBULLITION DU SODIUM DANS UN ECOULEMENT TURBULENT EN CANAL: EFFETS DU FLUX THERMIQUE ET DU DEBIT

**Résumé**—On a mené une étude expérimentale dans laquelle les effets du flux thermique et de la vitesse sur la surchauffe en début d'ébullition ont été déterminés pour un écoulement turbulent de sodium dans un canal annulaire. La surface chauffante polie est en acier inoxydable de type 316 ayant une rugosité, déterminée au profilomètre, entre 0,356 et 0,457 μm. On maintient constante la vitesse de croissance de la temperature de la surface chauffante dans chaque essai de début d'ébullition, en élevant graduellement la température d'entrée du sodium dans la section d'essai, tandis que l'on maintient constànt le flux thermique sur le chauffoir. De cette manière, les variables indépendantes, flux thermique et vitesse de croissance de la température, sont séparées.

Pour une vitesse finie de montée de température, on trouve que plus le flux thermique est grand, plus grande est la surchauffe en début d'ébullition, les autres choses restant égales par ailleurs. On a aussi constaté que plus la vitesse de croissance de la température est grande, plus important est l'effet du flux thermique. Ce flux varie entre 79 et 950 $kW/m^2$.

En accord général avec les résultats publies antérieurement, la surchauffe en début d'ébullition dépend fortement du débit, diminuant exponentiellement.

## ÜBERHITZUNG VON NATRIUM BEI SIEDEBEGINN IN TURBULENTER KANALSTRÖMUNG. DER EINFLUSS DER WÄRMESTROMDICHTE UND DER MASSENSTROMDICHTE

**Zusammenfassung**—In einer experimentellen Untersuchung wurde der Einfluss der Wärmestromdichte und der Geschwindigkeit auf die Überhitzung im Siedebeginn bei turbulent strömendem Natrium in einem Ringkanal bestimmt. Die Heizfläche bestand aus poliertem, rostfreiem 316-Stahl mit einer gemessenen Rauhigkeit von 350–450 $\mu m$ (RMS). Die Temperaturanstiegsrate der Heizfläche wurde bei jedem Siedeversuch konstant gehalten, indem die Temperatur des in die Versuchsstrecke eintretenden Natriums stetig erhöht wurde, während der Wärmestrom der Heizung konstant blieb. Auf diese Weise wurden die unabhängigen veränderlichen Grössen Wärmestrom und Temperaturanstieg getrennt.

Bei einem endlichen Anstieg der Temperatur zeigt sich, dass die Anfangsüberhitzung beim Sieden um so grösser ist, je grösser der Wärmestrom ist, solange andere Parameter gleich bleiben. Weiterhin wurde beobachtet, dass mit grösserem Temperaturanstieg der Einfluss des Wärmestroms wächst. Der Wärmestrom wurde zwischen 80 und 950 $kW/m^2$ variiert.

In Übereinstimmung mit veröffentlichten Ergebnissen früherer Untersuchungen wurde beobachtet, dass die Überhitzung bei Siedebeginn stark vom Massenstrom abhängt. Sie fällt exponentiell mit steigendem Massenstrom.

Der axiale Ort des Siedebeginns wurde durch eine Anzahl von Spannungsabgriffen entlang der äusseren Wand der Versuchsstrecke bestimmt. Die hier wiedergegebenen Ergebnisse liefern Überleitungswerte und Angaben zur Blasenbildung am oberen Teil der Heizstrecke oder an der Stelle der höchsten Temperatur der Heizfläche im Versuchskanal.

## ПЕРЕГРЕВ НА НАЧАЛЬНОЙ СТАДИИ КИПЕНИЯ НАТРИЯ ПРИ ЕГО ТУРБУЛЕНТНОМ ТЕЧЕНИИ В КАНАЛЕ В ЗАВИСИМОСТИ ОТ ТЕПЛОВОГО ПОТОКА И СКОРОСТИ ТЕЧЕНИЯ

**Аннотация**—Выполнено экспериментальное исследование, в котором влияние теплового потока и скорости течения на перегрев на начальной стадии кипения определялись для турбулентного течения натрия в кольцевом канале. Поверхностью нагрева служила полированная нержавеющая сталь, имеющая шероховатость поверхности от 14 до 18 микродюймов (средне-квадратичное значение). В каждом опыте по кипению скорость роста температуры поверхности нагрева поддерживалась постоянной путём постепенного увеличения температуры натрия на входе в опытный участок. Величина теплового потока на нагревателе также поддерживалась постоянной. Таким образом было разделено влияние теплового потока и скорости роста температуры на перегрев.

Для конечной скорости роста температуры найдено, что при прочих равных условиях перегрев при кипении тем больше, чем больше тепловой иоток. Показано также, что чем больше скорость роста температуры, тем большее влияние тепловой поток оказывает на перегрев. Величина теплового потока изменялась в диапазоне от 25000 до 300000 БТЕ/час кв. фут.

В полном соответствии с ранее опубликованными результатами найдено, что перегрев на начальной стадии кипения сильно зависит от скорости течения, уменьшаясь экспоненциально по мере увеличения скорости течения.

Аксиальное распределение источников кипения определялось измерением напряжений на токоотводах, расположенных на некотором расстоянии друг от друга вдоль внешней стенки опытного участка. В работе представлены значения перегрева и образования пузырьков, полученные в верхней части нагревателя, а для наибольшего значения температуры поверхности нагрева-значения, полученные в опытном участке канала.